

Lead-free piezoceramics with giant strain in the system $\text{Bi}_{0.5}\text{Na}_{0.5}\text{TiO}_3 - \text{BaTiO}_3 - \text{K}_{0.5}\text{Na}_{0.5}\text{NbO}_3$. II. Temperature dependent properties

Shan-Tao Zhang, Alain Brice Kouna, Emil Aulbach, Wook Jo, Torsten Granzow, Helmut Ehrenberg, and Jürgen Rödel

Citation: *Journal of Applied Physics* **103**, 034108 (2008); doi: 10.1063/1.2838476

View online: <http://dx.doi.org/10.1063/1.2838476>

View Table of Contents: <http://scitation.aip.org/content/aip/journal/jap/103/3?ver=pdfcov>

Published by the AIP Publishing

Articles you may be interested in

Large strain response based on relaxor-antiferroelectric coherence in $\text{Bi}_{0.5}\text{Na}_{0.5}\text{TiO}_3 - \text{SrTiO}_3 - (\text{K}_{0.5}\text{Na}_{0.5})\text{NbO}_3$ solid solutions

J. Appl. Phys. **116**, 184104 (2014); 10.1063/1.4901549

Origin of the large strain response in $(\text{K}_{0.5}\text{Na}_{0.5})\text{NbO}_3$ -modified $(\text{Bi}_{0.5}\text{Na}_{0.5})\text{TiO}_3 - \text{BaTiO}_3$ lead-free piezoceramics

J. Appl. Phys. **105**, 094102 (2009); 10.1063/1.3121203

Piezoresponse and ferroelectric properties of lead-free $[\text{Bi}_{0.5}(\text{Na}_{0.7}\text{K}_{0.2}\text{Li}_{0.1})_{0.5}]\text{TiO}_3$ thin films by pulsed laser deposition

Appl. Phys. Lett. **92**, 222909 (2008); 10.1063/1.2938364

Lead-free piezoceramics with giant strain in the system $\text{Bi}_{0.5}\text{Na}_{0.5}\text{TiO}_3 - \text{BaTiO}_3 - \text{K}_{0.5}\text{Na}_{0.5}\text{NbO}_3$. I. Structure and room temperature properties

J. Appl. Phys. **103**, 034107 (2008); 10.1063/1.2838472

Giant strain in lead-free piezoceramics $\text{Bi}_{0.5}\text{Na}_{0.5}\text{TiO}_3 - \text{BaTiO}_3 - \text{K}_{0.5}\text{Na}_{0.5}\text{NbO}_3$ system

Appl. Phys. Lett. **91**, 112906 (2007); 10.1063/1.2783200



Not all AFMs are created equal
Asylum Research Cypher™ AFMs
There's no other AFM like Cypher

www.AsylumResearch.com/NoOtherAFMLikeIt

OXFORD
INSTRUMENTS
The Business of Science®

Lead-free piezoceramics with giant strain in the system $\text{Bi}_{0.5}\text{Na}_{0.5}\text{TiO}_3\text{--BaTiO}_3\text{--K}_{0.5}\text{Na}_{0.5}\text{NbO}_3$. II. Temperature dependent properties

Shan-Tao Zhang,¹ Alain Brice Kounga,¹ Emil Aulbach,¹ Wook Jo,^{1,a)} Torsten Granzow,¹ Helmut Ehrenberg,² and Jürgen Rödel¹

¹*Institute of Materials Science, Technische Universität Darmstadt, Petersenstr. 23, 64287 Darmstadt, Germany*

²*Institute for Complex Materials, IFW Dresden, Helmholtzstr. 20, 01069 Dresden, Germany*

(Received 10 September 2007; accepted 2 December 2007; published online 12 February 2008)

The temperature dependence of the dielectric and ferroelectric properties of lead-free piezoceramics of the composition $(1-x-y)\text{Bi}_{0.5}\text{Na}_{0.5}\text{TiO}_3-x\text{BaTiO}_3-y\text{K}_{0.5}\text{Na}_{0.5}\text{NbO}_3$ ($0.05 \leq x \leq 0.07$, $0.01 \leq y \leq 0.03$) was investigated. Measurements of the polarization and strain hystereses indicate a transition to predominantly antiferroelectric order when heating from room temperature to 150 °C, while for $150 < T < 200$ °C both remnant polarization and coercive field increase. Frequency-dependent susceptibility measurements show that the transition is relaxorlike. For some samples, the transition temperature T_d is high enough to allow mostly ferroelectric ordering at room temperature. These samples show a drastic increase of the usable strain under an external electric field just after the transition into the antiferroelectric state at high temperatures. For the other samples, T_d is so low that they display significant antiferroelectric ordering already at room temperature. In these samples, the usable strain is relatively stable over a wide temperature range. In contrast to T_d , the temperature T_m of the transition into the paraelectric high-temperature phase depends far less on the sample composition. These results confirm that the high strain in this lead-free system is due to a field-induced antiferroelectric-ferroelectric phase transition and that this effect can be utilized in a wide temperature range. © 2008 American Institute of Physics. [DOI: 10.1063/1.2838476]

I. INTRODUCTION

Piezoelectric ceramic materials are widely used in electronic devices such as sensors and actuators under various working environments. As a consequence, knowledge of the materials' properties under the specific working conditions is crucial for the design of piezoelectric devices. Most notably, this includes the temperature during operation of piezoelectric devices, which can range from hot like in combustion engines to very cold like those occurring in aerospace applications. Recent investigations of the temperature variation of the properties of the ubiquitous piezoelectric ceramic system $\text{Pb}(\text{Zr},\text{Ti})\text{O}_3$ (PZT) in the range from 4.2 to 675 °K have revealed that the material properties and consequently the performance of the devices at the working environment can differ significantly from those at ambient temperature.^{1–5}

Due to the toxicity of the heavy metal lead, much effort is being put into the search of lead-free piezoelectric ceramics that can eventually replace PZT-based materials in all applications. One focus has been directed toward perovskite-type ferroelectric systems based on $\text{Bi}_{0.5}\text{Na}_{0.5}\text{TiO}_3$ (BNT), $\text{K}_{0.5}\text{Na}_{0.5}\text{NbO}_3$ (KNN), BaTiO_3 (BT), and mixed systems of these end members.^{6–10} It has been shown that these lead-free piezoceramics exhibit good piezoelectric responses for compositions near the morphotropic phase boundary between phases belonging to different crystal classes. However,

there are not many reports of the effect of temperature on BNT- or KNN-based piezoceramics in the literature.^{6,10,11}

It is well known that BNT-rich lead-free piezoceramics undergo a transition from a ferroelectric (FE) low-temperature phase to an antiferroelectric (AFE) high-temperature phase at a certain depolarization temperature T_d .^{12–14} In the vicinity of T_d , the piezoelectric performance may be enhanced, since the strain response can have two separate contributions: an extrinsic contribution due to ferroelectric non-180° domain switching and an intrinsic contribution due to changes in the dimensions of the crystal lattice.^{15,16} Indeed, an extremely high strain was observed in lead-free piezoceramics especially with the composition of 0.92BNT-0.06BT-0.02KNN in our previous work.¹⁷ It was proposed that these systems contain a mixture of FE and AFE phases and the high strain was in large part attributed to an AFE-FE phase transition induced by the externally applied electric field.¹⁷ This proposed mechanism was strongly supported by the investigation of the nearby compositions of 0.92BNT-0.06BT-0.02KNN.¹⁸ Since the stability of AFE phase depends not only on composition but also on temperature, we investigated the temperature-dependent properties of all the compositions we explored in our previous work¹⁸ to manifest the hypothesis of a phase transition as the origin of its uniquely large strains and to evaluate the suitability of the recently developed lead-free system for applications in a wider temperature range.

^{a)}Author to whom correspondence should be addressed. Electronic mail: jo@ceramics.tu-darmstadt.de.

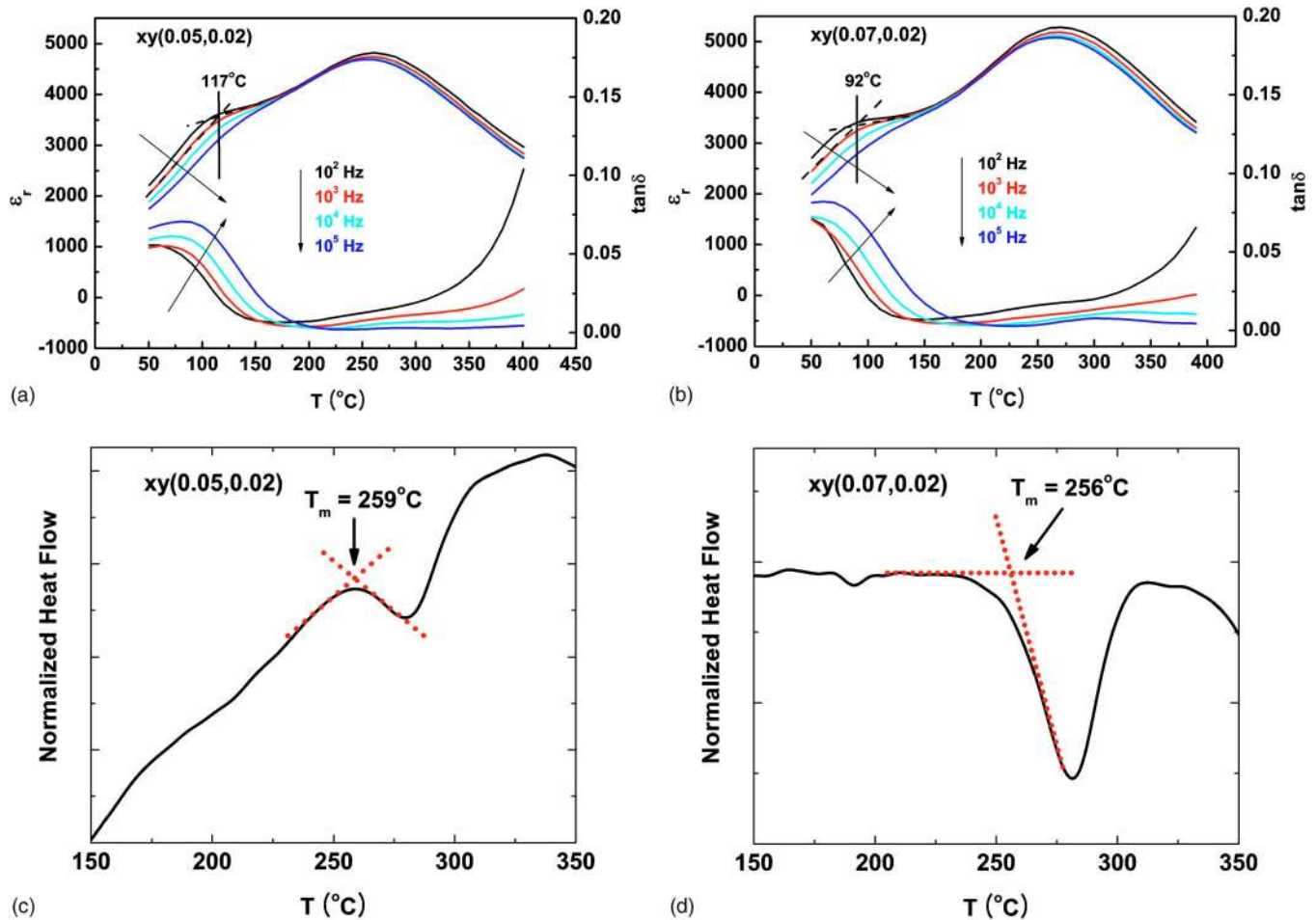


FIG. 1. (Color online) Temperature dependent ϵ_r and $\tan \delta$ of (a) 0.93BNT-0.05BT-0.02KNN and (b) 0.91BNT-0.07BT-0.02KNN, together with the differences of heat flows in two successive DSC runs on (c) 0.93BNT-0.05BT-0.02KNN and (d) 0.91BNT-0.07BT-0.02KNN.

II. EXPERIMENTS

Details of the procedures for the sample preparation were the same as reported in the previous papers.^{17,18} We measured the temperature dependent dielectric, ferroelectric, and piezoelectric properties of $(1-x-y)\text{BNT}-x\text{BT}-y\text{KNN}$, where $0.05 \leq x \leq 0.07$ and $0.01 \leq y \leq 0.03$.¹⁸ Relative dielectric permittivity and loss of unpoled ceramics were measured using an impedance analyzer (HP4284A, Hewlett-Packard Company) in the frequency range from 100 Hz to 1 MHz in a temperature range from 50 to 400 $^{\circ}\text{C}$. In addition, to confirm both depolarization and paraelectric transition, differential scanning calorimetric (DSC) measurements (Perkin Elmer Diamond) were performed from room temperature up to 400 $^{\circ}\text{C}$ under Ar atmosphere at a heating/cooling rate of 20 $^{\circ}\text{C}/\text{min}$. Measurements of the ferroelectric polarization and strain hysteresis [$P(E)$ and $S(E)$, respectively] were performed in a silicone oil bath at a frequency of 50 mHz for $25 \leq T \leq 200$ $^{\circ}\text{C}$ with temperature steps of 25 $^{\circ}\text{C}$. The strain was measured by means of a linear variable differential transformer encapsulated in an alumina tube, which ensured thermal and electrical insulation and reliable response at elevated temperatures. A Sawyer–Tower circuit was used to measure the change of the polarization during the application of an electric field. The field amplitude was 6 kV/mm.

III. RESULTS AND DISCUSSION

Figures 1(a) and 1(b) exemplarily show the temperature-dependent relative dielectric constant (ϵ_r) and dielectric loss ($\tan \delta$) of 0.93BNT-0.05BT-0.02KNN and 0.91BNT-0.07BT-0.02KNN, respectively. All $\epsilon_r(T)$ -curves display two notable features. We attribute the shoulder at lower temperatures to a FE-AFE phase transition and designate its onset point as the depolarization temperature T_d . The more clearly defined maximum at the higher temperatures T_m is attributed to the transition into the paraelectric high-temperature phase. Both features are rather diffuse, and the position of T_d exhibits a notable dependence on the measurement frequency, indicating a relaxor-type transition.¹⁹ T_m is almost frequency independent for all compositions, which is consistent with a literature report on BNT-based ceramics with a low level of dopants or substitution.¹⁰

To further confirm the presence of both transitions, DSC analyses were performed. Although no peaks are obvious in the temperature dependence of the heat flow, clear signals become evident in the difference curves of two successive heat runs ($\text{RT} \rightarrow 400$ $^{\circ}\text{C} \rightarrow 40$ $^{\circ}\text{C} \rightarrow 400$ $^{\circ}\text{C}$) on the same sample without relaxation period in between at 40 $^{\circ}\text{C}$. Difference curves are presented in Figs. 1(c) and 1(d). While no peaks for the rather weak transitions T_d are detected, signals

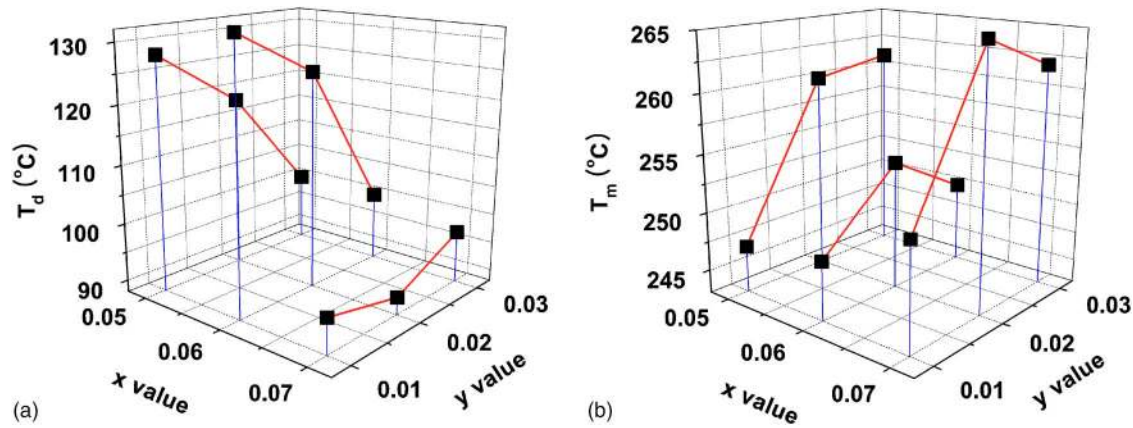


FIG. 2. (Color online) Composition dependent (a) T_d and (b) T_m measured at a frequency of 1 kHz. T_d of the compositions with dominant ferroelectric order at RT (group I) is generally higher than that with mixed ferroelectric and antiferroelectric order at RT (group II), whereas T_m exhibits little dependence on composition.

corresponding to T_m are observed near 260 °C, regardless of the composition of the samples, consistent with results from the dielectric measurements. The high-temperature phases above T_m remain metastable at 40 °C, so that base lines without phase transitions at T_m are recorded in the second runs, and the weak signals corresponding to the phase transitions are revealed in the difference curves. A relaxation period of 2 h at 40 °C is sufficient for a sample to return from the metastable high-temperature phase into the ambient-condition phase. In Fig. 2, T_d and T_m measured at 1 kHz are plotted as a function of sample composition. As noted before, based on piezoelectric measurements,^{17,18} samples can be roughly divided into two groups: samples with low BT and KNN contents (group I) exhibit predominant FE ordering at room temperature, while samples with high BT or KNN content (group II) display predominantly AFE behavior. This classification still persists with temperature-dependent properties, albeit less clearly. Materials from group I tend to have a higher T_d , while samples from group II have lower T_d .

Figures 3(a) and 3(b) exemplarily show the polarization hysteresis $P(E)$ of 0.93BNT-0.05BT-0.02KNN and 0.91BNT-0.07BT-0.02KNN, respectively, for three temperatures. For 0.93BNT-0.05BT-0.02KNN, the $P(E)$ loop at RT is saturated and exhibits a shape typical for ferroelectrics.

When the temperature is increased to 75 °C, the polarization at high fields remains nearly unchanged, but the remnant polarization P_r and the coercive field E_c drop sharply. As a result, the hysteresis loop becomes “pinched,” reminiscent of that of antiferroelectric materials. It has to be noted that this starts to occur far below T_d determined by dielectric measurements, a fact that is attributed to the broadness and frequency dependence of the transition. Apparently, at a frequency of 50 mHz, the AFE order seems to dominate even in 0.93BNT-0.05BT-0.02KNN. The antiferroelectric features become even more pronounced at higher temperatures. A similar development is observed for 0.91BNT-0.07BT-0.02KNN, but here the room-temperature curve already shows antiferroelectric characteristics, again far below the T_d determined for this composition.

Figure 4 shows the development of the characteristic parameters P_r and E_c with temperature for all compositions. E_c and P_r decreased continuously with increasing temperature up to 150 °C. At this temperature, all materials are in the antiferroelectric phase, as shown in Fig. 1. A determination of P_r and E_c for higher temperatures thus does not mean; furthermore, $P(E)$ -measurements at higher temperatures were seriously impeded by electrical leakage through the samples. As was expected, the changes of the ferroelectric behavior of the samples indicated in Fig. 4 are closely

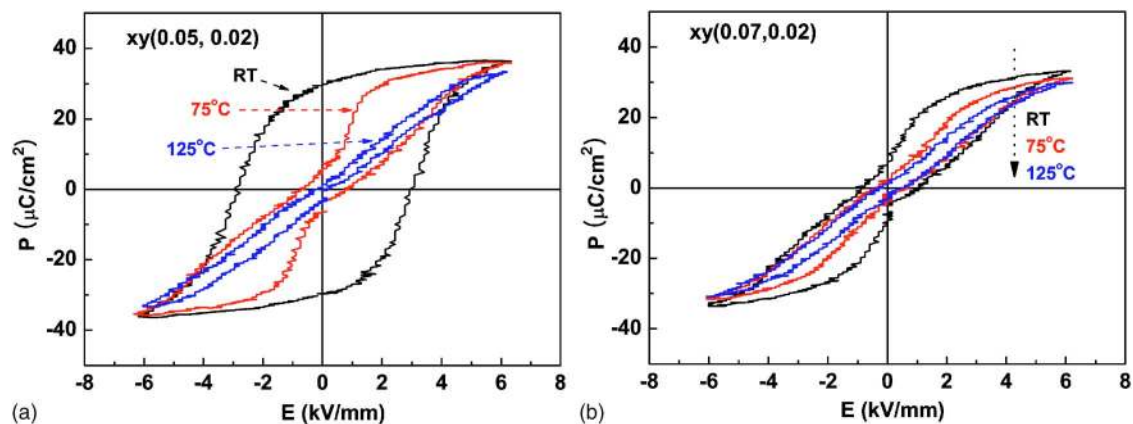
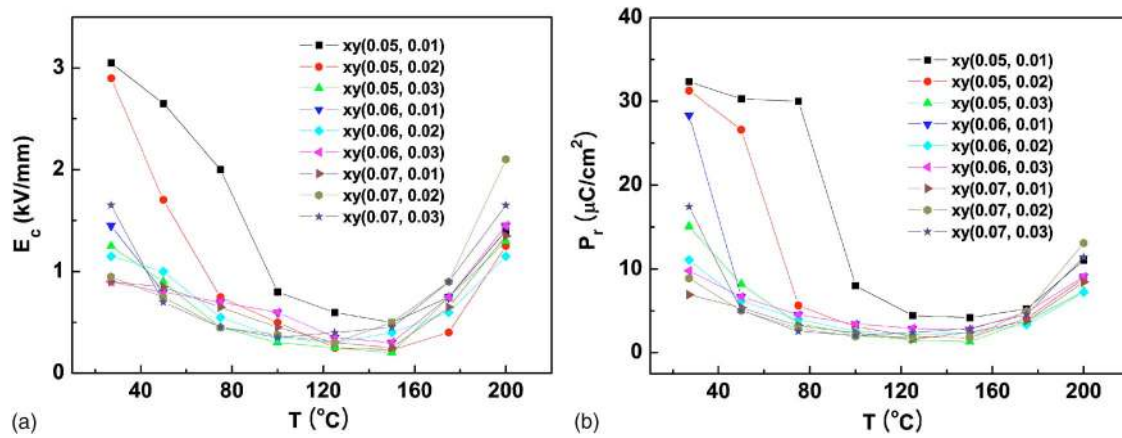


FIG. 3. (Color online) Temperature dependent $P(E)$ loops of (a) 0.93BNT-0.05BT-0.02KNN and (b) 0.91BNT-0.07BT-0.02KNN.

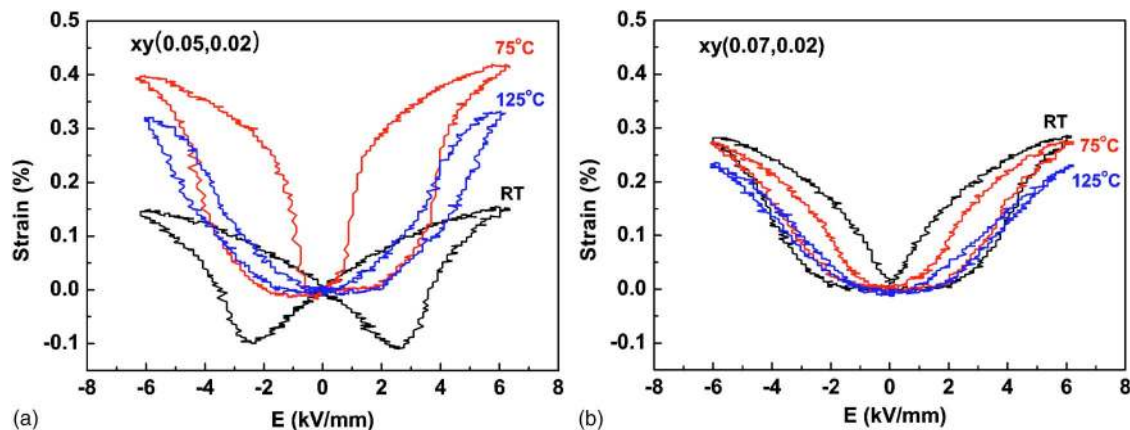
FIG. 4. (Color online) Temperature dependent (a) E_c and (b) P_r for all compositions.

correlated to their respective depolarization temperature as seen in Fig. 2. Again, a distinction between samples that show predominantly ferroelectric behavior at room temperature (group I), particularly compositions with 5% BT, and those with predominantly antiferroelectric behavior (group II) is visible.

The most important feature of piezoelectrics is of course the strain that can be achieved with an electric field. Therefore, Figs. 5(a) and 5(b) show the bipolar $S(E)$ curves of 0.93BNT-0.05BT-0.02KNN and 0.91BNT-0.07BT-0.02KNN, respectively, at three temperatures. At RT, the $S(E)$ curve of 0.93BNT-0.05BT-0.02KNN has a butterfly shape, again typical for materials with dominant ferroelectric order. This shape gradually changes with increasing temperature: the lower parts of the curves become flatter, and the “negative strain,” i.e., the difference between the strain at zero field and the minimum of the $S(E)$ -curve,¹⁸ vanishes. Above 75 °C, there is no strain for low electric fields; high fields are required to induce a notable strain. This behavior can again be traced to the development of antiferroelectric ordering at high temperatures, where the strain can only be changed after a field-induced transition back to the ferroelectric state. Similar results were also observed in both Pb-based antiferroelectric materials and BNT-BT single crystals.^{20–25} It has to be noted that the total strain, i.e., the difference between the

maximum and minimum of $S(E)$, increases between room temperature and T_d ; apparently, the field-induced phase transition leads to a large distortion of the crystal lattice, and correspondingly to a strain that is even higher than that which can be reached by the “normal” piezoelectric effect (domain switching plus lattice extension) in the low-temperature ferroelectric phase. As was expected, a further increase in temperature up to 200 °C did not change the shape of the curve anymore, but the total strain receded again. Once more, group II compositions behave likewise, but already start off in the AFE phase at room temperature. To characterize the changes in the loop shape, Fig. 6 depicts the temperature dependence of the negative strain of all compositions. It generally decreases with increasing temperature and is practically zero above the corresponding T_d . Again, the shape of the $S(E)$ curves of group I compositions has a stronger dependence on temperature than that of the group II compositions.

Since most piezoelectric actuators are driven with a unipolar voltage, we also investigated the temperature dependence of unipolar $S(E)$ -curves. Figure 7 exemplarily displays the results for 0.93BNT-0.05BT-0.02KNN and 0.91BNT-0.07BT-0.02KNN. The trend of the bipolar strain curves is reproduced here: for 0.93BNT-0.05BT-0.02KNN, the maximum unipolar strain S_{\max} increases when the temperature is

FIG. 5. (Color online) Temperature dependent bipolar $S(E)$ curves of (a) 0.93BNT-0.05BT-0.02KNN and (b) 0.91BNT-0.07BT-0.02KNN. The shape and maximum strain of 0.93BNT-0.05BT-0.02KNN change more significantly than that of 0.91BNT-0.07BT-0.02KNN.

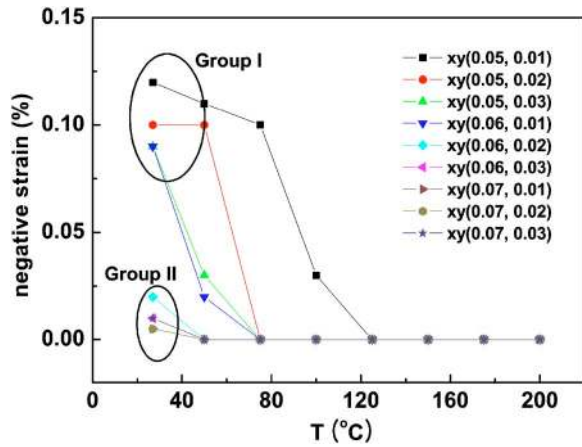


FIG. 6. (Color online) Temperature dependent negative strain under bipolar field loading, showing that the shape change in the $S(E)$ curve of group I compositions is more significant than that of group II compositions.

increased from RT to 75 °C, remains practically constant up to 100 °C, and then drops considerably with a further increase in temperature. We also note that the hysteresis of the unipolar $S(E)$ curve increases when heating from RT to 75 °C, then decreases again. This effect is also related to the field-induced AFE-FE phase transition.^{18–23}

In the case of 0.91BNT-0.07BT-0.02KNN, however, S_{\max} as well as the hysteretic behavior decrease smoothly in the whole temperature range. To compare all samples, the temperature dependence of S_{\max} is provided for all compositions in Fig. 8. Figure 9 gives a better visual impression of the dependence of S_{\max} on composition at four selected temperatures in a three-dimensional plot. At room temperature, S_{\max} of group I compositions is about two times lower than that of group II compositions. With increasing temperature, S_{\max} of group I compositions increases, while that of group II compositions decreases. For example, at 50 °C, S_{\max} of 0.92BNT-0.05BT-0.03KNN and 0.93BNT-0.06BT-0.01KNN are comparable to the values of the material reported in Ref. 17, while 0.94BNT-0.05BT-0.01KNN and 0.93BNT-0.05BT-0.02KNN exhibit a poorer performance. However, when temperature reaches 100 °C, S_{\max} of group I compositions especially 0.94BNT-0.05BT-0.01KNN and 0.93BNT-

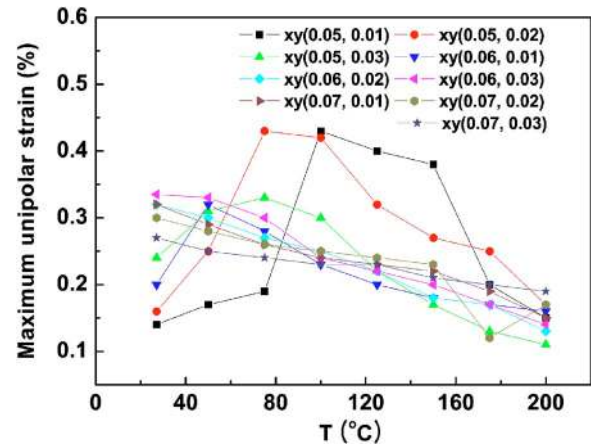


FIG. 8. (Color online) Temperature dependent maximum unipolar strain values for all compositions.

0.05BT-0.02KNN is two times larger than that of group II compositions. A further increase of the temperature up to 200 °C led to a decrease in S_{\max} for all compositions. It is also noted that for 0.94BNT-0.05BT-0.01KNN, S_{\max} reaches 0.43%, corresponding to a large-field piezoelectric coefficient S_{\max}/E_{\max} of 700 pm/V at 100 °C and changes only little up to 150 °C. This S_{\max}/E_{\max} value is higher than any reported values of other lead-free and untextured lead-containing polycrystalline ferroelectric ceramics.^{17,18}

The temperature dependence of all properties investigated supports the hypothesis that the examined samples can be grouped into two categories: those that display predominantly ferroelectric order and those that display predominantly antiferroelectric order at room temperature. When increasing the temperature, the prevalence of antiferroelectric order increases in all samples, leading to drastic changes in the behavior of group I samples, but only slight changes in group II materials. There are little or no remnants of ferroelectric order above 150 °C. However, the ferroelectric order appears to decrease far below the expected depolarization temperature T_d in all samples. The strain that can be reached by applying an electric field reaches its maximum near the point where the balance tips in favor of the antiferroelectric order. This is a clear proof that the mechanism by which the

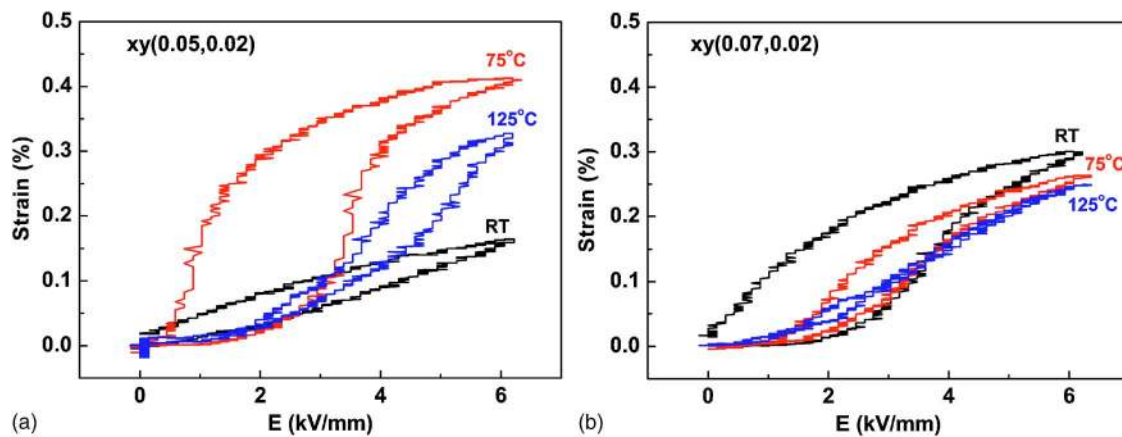


FIG. 7. (Color online) Temperature dependent unipolar $S(E)$ curves of (a) 0.93BNT-0.05BT-0.02KNN and (b) 0.91BNT-0.07BT-0.02KNN. Note that the hysteresis and maximum strain have different temperature dependences.

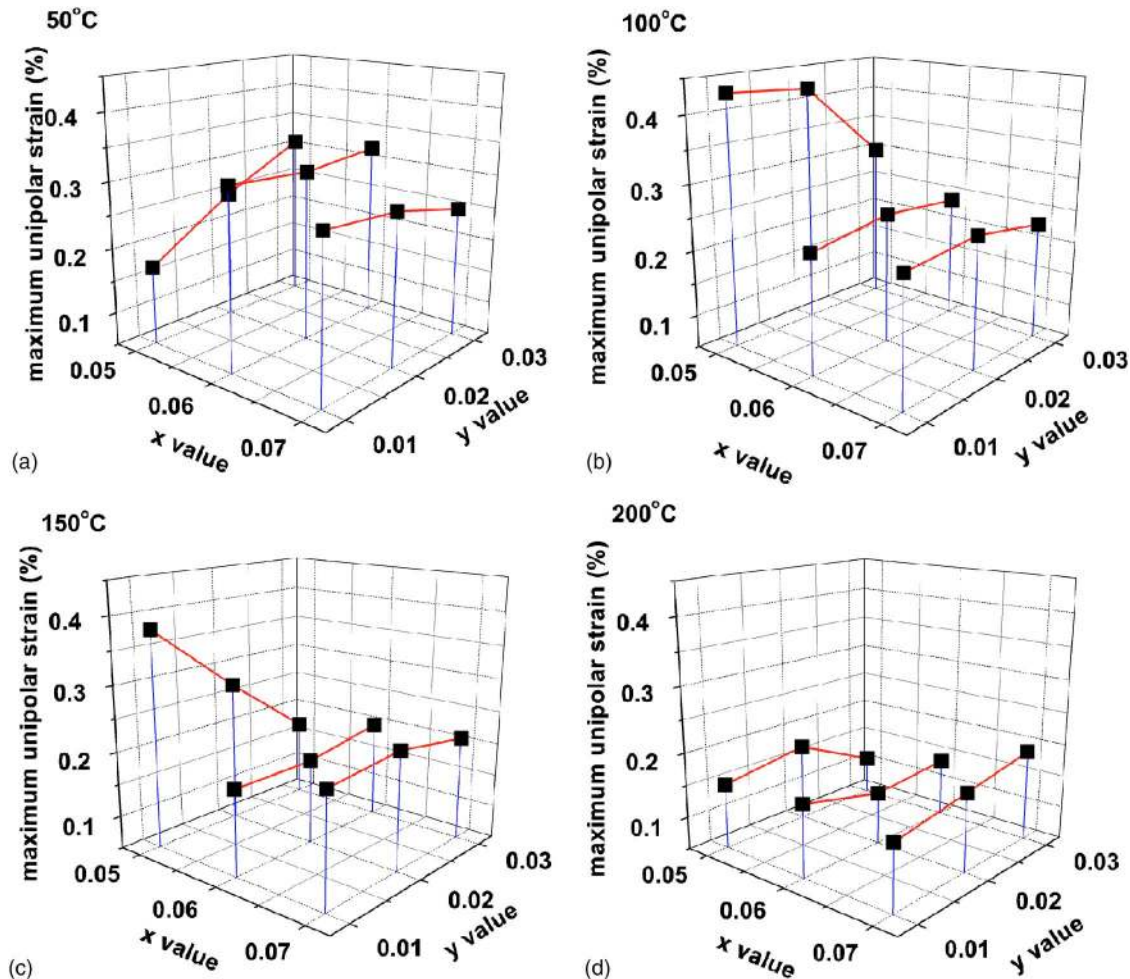


FIG. 9. (Color online) Three-dimensional plots of maximum strain value at (a) 50 °C, (b) 100 °C, (c) 150 °C, and (d) 200 °C.

strain is created is not normal piezoelectricity, which occurs only in the ferroelectric phase, but is carried in large parts by the AFE-FE phase transition induced by the external field, coupled with reorientation of the remaining ferroelectric domains.

IV. CONCLUSION

In summary, the dielectric, ferroelectric and piezoelectric properties of $(1-x-y)\text{BNT}-x\text{BT}-y\text{KNN}$ ($0.05 \leq x \leq 0.07$ and $0.01 \leq y \leq 0.03$) lead-free piezoceramics were investigated in the temperature range $25 \leq T \leq 200$ °C. The dielectric spectra suggest the existence of a depolarization temperature T_d , corresponding to a transition from a ferroelectric to an antiferroelectric phase, and a temperature T_m indicating a transition from the antiferroelectric to a paraelectric phase. The different values of T_d led to different temperature dependent properties, such as P_r , E_C , strain loop shape, and maximum strain. The high strain was explained in terms of the field induced antiferroelectric-ferroelectric phase transition. At high temperatures, the field-induced phase transition needed higher fields, leading to a decrease in the total observed strain. These results are helpful to further understand the high strain in lead free BNT-BT-KNN-based systems and at the same time indicate a good temperature stability of the piezoelectric properties above T_d .

ACKNOWLEDGMENTS

This work was supported by the Deutsche Forschungsgemeinschaft (DFG) under SFB 595. S.T.Z thanks the Alexander von Humboldt foundation for financial support. We acknowledge support by B. Bartusch (IFW Dresden) for the DSC measurements.

- ¹X. L. Zhang, Z. X. Chen, L. E. Cross, and W. A. Schulze, *J. Mater. Sci.* **18**, 968 (1983).
- ²D. Wang, Y. Fotinich, and G. P. Carman, *J. Appl. Phys.* **83**, 5342 (1998).
- ³Q. M. Zhang, H. Wang, N. Kim, and L. E. Cross, *J. Appl. Phys.* **75**, 454 (1994).
- ⁴I. Franke, K. Roleder, L. Mitoseriu, R. Piticescu, and Z. Ujma, *Phys. Rev. B* **73**, 144114 (2006).
- ⁵H. Kungl and M. J. Hoffmann, *Acta Mater.* (in press).
- ⁶Y. Saito, H. Takao, T. Tani, T. Nonoyama, K. Takatori, T. Homma, T. Nagaya, and M. Nakamura, *Nature (London)* **432**, 84 (2004).
- ⁷E. Hollenstein, M. Davis, D. Damjanovic, and N. Setter, *Appl. Phys. Lett.* **87**, 182905 (2005).
- ⁸S. J. Zhang, R. Xia, T. R. Shrout, Z. G. Zang, and J. F. Wang, *J. Appl. Phys.* **100**, 104108 (2006).
- ⁹T. R. Shrout and S. J. Zhang, *J. Electroceram.* **19**, 113 (2007).
- ¹⁰T. Takenaka, K. Maruyama, and K. Sakata, *Jpn. J. Appl. Phys., Part 1* **30**, 2236 (1991).
- ¹¹Y. Hiruma, Y. Makiuchi, R. Aoyagi, H. Nagata, and T. Takenaka, *Ceram. Trans.* **174**, 139 (2006).
- ¹²Y. Hiruma, H. Nagata, and T. Takenaka, *Jpn. J. Appl. Phys., Part 1* **45**, 7409 (2006).
- ¹³X. X. Wang, X. G. Tang, and H. L. W. Chan, *Appl. Phys. Lett.* **85**, 91 (2004).

- ¹⁴T. Oh, Jpn. J. Appl. Phys., Part 1 **45**, 5138 (2006).
- ¹⁵J. L. Jones, M. Hoffman, J. E. Daniels, and A. J. Studer, Appl. Phys. Lett. **89**, 092901 (2006).
- ¹⁶H. Kungl, T. Fett, S. Wagner, and M. J. Hoffmann, J. Appl. Phys. **101**, 044101 (2007).
- ¹⁷S. T. Zhang, A. B. Kounga, E. Aulbach, H. Ehrenberg, and J. Rödel, Appl. Phys. Lett. **91**, 112906 (2007).
- ¹⁸S. T. Zhang, A. B. Kounga, E. Aulbach, T. Granzow, W. Jo, H.-J. Kleebe, and J. Rödel, J. Appl. Phys. **103**, 034108 (2008).
- ¹⁹G. A. Samara, J. Phys.: Condens. Matter **15**, R367 (2003).
- ²⁰R. P. Brodeur, K. W. Gachigi, P. M. Pruna, and T. R. Shrout, J. Am. Ceram. Soc. **77**, 3042 (1994).
- ²¹S. E. Park, M. J. Pan, K. Markowski, S. Yoshikawa, and L. E. Cross, J. Appl. Phys. **82**, 1798 (1997).
- ²²C. Heremans and H. L. Tuller, J. Appl. Phys. **87**, 1458 (2000).
- ²³Y. W. Nam and K. H. Yoon, Mater. Res. Bull. **36**, 171 (2001).
- ²⁴Y. J. Yu and R. N. Singh, J. Appl. Phys. **94**, 7250 (2003).
- ²⁵Y. M. Chiang, G. W. Farrey, and A. N. Soukhojak, Appl. Phys. Lett. **73**, 3683 (1998).